Materials Science and Technology

ISSN: 0267-0836 (Print) 1743-2847 (Online) Journal homepage: http://www.tandfonline.com/loi/ymst20

Structure and properties of strengthening layer on Hardox 450 steel

Yurii Ivanov, Victor Gromov, Sergey Konovalov , Vasilii Kormyshev, Krestina Aksenova & Anton Teresov

To cite this article: Yurii Ivanov, Victor Gromov, Sergey Konovalov , Vasilii Kormyshev, Krestina Aksenova & Anton Teresov (2017): Structure and properties of strengthening layer on Hardox 450 steel, Materials Science and Technology, DOI: 10.1080/02670836.2017.1343231

To link to this article: http://dx.doi.org/10.1080/02670836.2017.1343231

Published online: 05 Jul 2017.

MATERIALS SCIENCE AND TECHNOLOGY, 2017
https://doi.org/10.1080/02670836.2017.1343231

The Institute of Materials, Minerals and Mining
Taylor & Francis
Taylor & Francis Group

Structure and properties of strengthening layer on Hardox 450 steel

Yurii Ivanov[a], Victor Gromov[b], Sergey Konovalov [b,c], Vasilii Kormyshev[b], Krestina Aksenova[b] and Anton Teresov[a]

[a]Institute of High-Current Electronics of Siberian Branch of Russian Academy of Sciences, Tomsk, Russia; [b]Siberian State Industrial University, Novokuznetsk, Russia; [c]Samara National Research University, Samara, Russia

ABSTRACT
The microstructure and microhardness distribution in the surface of low-carbon Hardox 450 steel coated with alloyed powder wires of different chemical compositions are studied. It is shown that the microhardness of 6–8 mm-thick surfaced layer exceeds that of base metal by more than two times. The increased mechanical properties of surfaced layer are caused by the submicro and nanoscale dispersed martensite, containing the niobium carbides Nb_2C, NbC and iron borides Fe_2B. In the bulk plates, a dislocation substructure of the net-like type with scalar dislocation density of 10^{11} cm^{-2} is observed. The layer surfaced with the wire containing B possesses highest hardness. The possible mechanisms and temperature regimes of niobium and boron carbides in surfacing are discussed.

ARTICLE HISTORY
Received 29 March 2017
Revised 4 June 2017
Accepted 6 June 2017

KEYWORDS
Nanostructure; phase constitution; microhardness; electro arc surfacing; eutectic; boron carbides; niobium carbides

Introduction

Surface coatings open up new possibilities to manipulate materials with requirable properties in particular environments. Protective coating layer can be achieved using thermal spraying, cladding and welding [1–6]. Among all the available methods, welding is considered to be an economical one as a variety of processes can be implemented to deposit the desired coatings. In most cases, a wire is used as an electrode or filler to form a protective layer on the surface of a base metal.

Among the weld cladding procedures, gas tungsten arc (GTA) surfacing process is a cost-effective approach applied when reactive materials (as coatings or substrates) are involved [7–9]. GTA surface modification by means of alloying is a process in which an alloy powder of a desirable composition and a thin surface layer of the substrate material are simultaneously melted, and then rapidly solidified to form a dense coating metallurgically bonded to the base material [10]. The solidification rate is very high during coating in this process. Moreover, the coated surface obtained by GTA technique has the potential to produce rapidly solidified fine microstructures that has high hardness and wear resistance synthesised on various traditional substrate materials [11,12].

The effects of GTA processing were used for developing wear resistance of AISI 1020 steel substrate. Appropriate quantities of FeB powder and Hardox 450 steel were combined to create conditions that synthesise particles into reinforced Fe-based composite surface coating [13]. The studies concluded that Hardox 450 steel + 40 wt-% FeB composite coating was the most appropriate combination in terms of hardness and wear performance [13].

Hardox 450 steel is used to generate desirable wear resistance and excellent cold bending property and weldability. High hardness Hardox 450 steel is obtained by quenching a sheet with special composition to generate martensite structure. To improve its technological properties further, the steel underwent additional modification including surface processing for obtaining the demanded properties [14–18].

The purpose of this research was to analyse the phase constitution, defect substructure and mechanical properties of the layer surfaced on Hardox 450 steel with surfacing wire of different compositions.

Material and methods of research

The base material used was 16 mm-thick Hardox 450 sheet, and the filling wire used was 2 mm-diameter steel, whose chemical compositions are given in Tables 1 and 2. Before welding, the sheets were milled as 400 mm (length) × 200 mm (width) × 16 mm (thickness), and cleaned using acetone. The welding system was composed of a device PHOENIX 505 PROGRESS PULS. In the experiments, metal inert/active gas process was used to perform the surfacing. The welding conditions are shown in Table 3. For all experiments, the welding parameters are identical, and the inter-pass temperature was controlled to be lower than 120°C.

CONTACT Sergey Konovalov ksv@ssau.ru Siberian State Industrial University, Novokuznetsk 654007, Russia; Samara National Research University, Samara 443086, Russia

Table 1. Elemental composition of Hardox 450 steel (chemical composition of base metal, wt-%, balance Fe).

C	Si	Mn	Cr	Ni	Mo	B	P	S
0.19–0.26	0.70	1.60	0.25	0.25	0.25	0.004	0.025	0.010

Table 2. Elemental composition of electrode wire (wt-%, balance Fe).

	Elemental composition								
Wire identification	C	Mn	Si	Cr	Nb	W	Ni	B	V
1	1.3	0.9	1.1	7.0	8.5	1.4	0.0	0.0	0.0
2	0.7	2.0	1.0	0.0	0.0	0.0	2.0	4.5	0.0
3	1.4	0.0	0.0	7.0	8.0	1.2	0.0	0.0	1.0

Table 3. Welding parameters used in each surfacing and inter-pass temperature.

Welding current (A)	Arc voltage (V)	Welding speed (mm min^{-1})	Inter-pass temperature (°C)
250–300	30–35	110	< 120

The formation of surfaced layer was processed in atmosphere gas (98%Ar and 2%CO_2). All samples were polished to achieve mirror-like surfaces by removing a layer of up to $\sim$0.1 mm from each surface before recording the measurements. The Vickers microhardness values, HV, were obtained at room temperature using an PMT-3 microhardness instrument equipped with a Vickers indenter using a load of 5 N with a dwell time of 10 s for each separate measurement. The hardness values were recorded as the average of five positions formed in a cross-shape around each selected point at distances of 0.15 mm. The defect substructure of Hardox 450 steel and the surfaced layer was analysed using diffraction electron microscopy (DEM, EM-125). The foils are produced via electrolytic thinning of samples, cutting out the deposited metal (coating) and the steel spaced 15 mm from the contact area.

Results and discussion

Hardox 450 steel – initial state

DEM reveals the presence of lamellar crystals, as illustrated in Figure 1. It is a result of shear $\gamma \rightarrow \alpha$ transformation [19]. α-phase is iron-based solid solution with body-centred cubic (bcc) crystal lattice. The α-phase crystals are fragmental and separated into weakly disoriented, as shown in Figure 1(b). A small amount of sub-grains is present in the materials, as shown in Figure 2. Some secondary phases are found inside the plates and also around its boundaries, at boundaries of fragments and sub-grains, as shown in Figures 1(a,b) and 2. Those particles are Fe_3C according to the indexing of micro-electron diffraction patterns.

Mechanical properties of the surfaced layer

The microhardness profile of the steel surfaced layer was measured. The data plotted in Figure 3 show that as a result of surfacing formation (independent of surfacing wire grade), a high-strength surface layer not less than 6 mm thickness with average value of microhardness $\approx$11.2 GPa is formed. When moving farther away from the surfaced layer, the microhardness of the material drops quickly into a level of $\approx$5.8 GPa. Consequently, the hardness of surfaced layer exceeds that of the base metal (Hardox 450 steel) by 1.9 times in a thickness of 6.0–8.0 mm. The highest hardness is the layer surfaced with wire No.2 shown as the curve 1 in Figure 3. In this case, the hardened layer thickness is not less than 7.5 mm. Its microhardness varies between 10.5 and 12.5 GPa.

Phase constitution of the defect substructure in surfaced layer

By analysing the composition of surfacing wire presented in Table 2, it can be supposed that high strength properties of the layer surfaced with wire No.2 are caused by hardening of the material with iron boride.

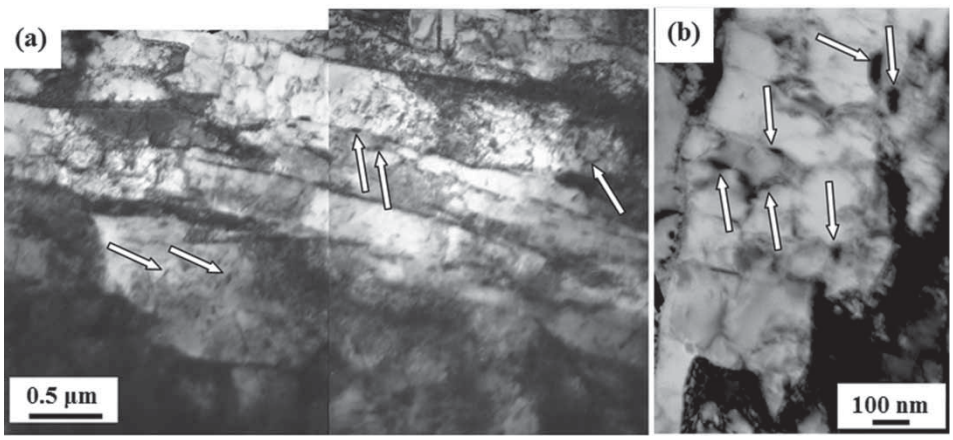

Figure 1. Electron microscope image of Hardox 450 steel structure; the arrows designate the particles of carbide phase.

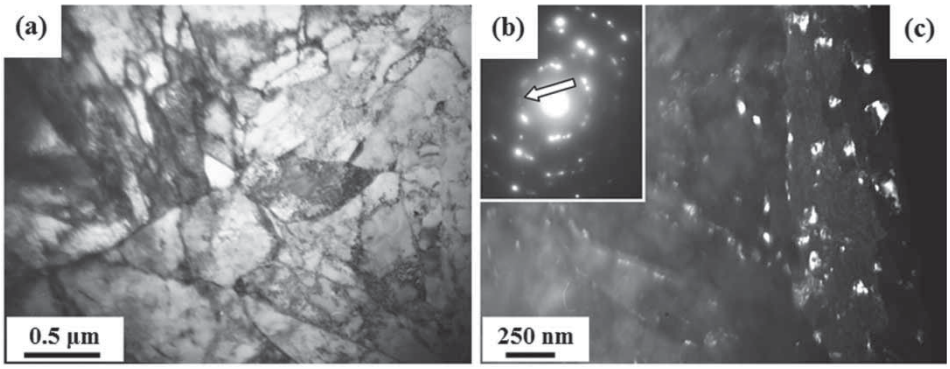

Figure 2. Electron microscope image of Hardox 450 steel; (a) light field; (b) micro-electron diffraction pattern to (a) and (c) dark field image obtained in reflection [031]Fe_3C (the arrow designates the reflection in (b)).

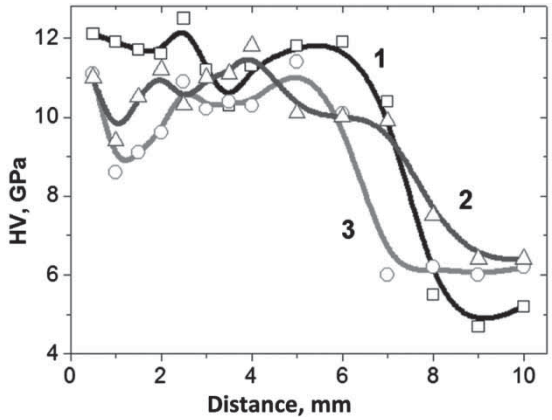

Figure 3. Microhardness profile of 'surfaced layer/(Hardox 450 steel) substrate'; curve 1 – surfacing wire No.2; curve 2 – surfacing wire No.3; curve 3 – surfacing wire No.1.

Fe–B system contains the compounds of Fe_2B, FeB and FeB_2. The solubility of boron in α-Fe is 0.008% (at.) at 906°C and is smaller in γ-Fe [20]. In Fe–B–C ternary systems, it is possible to form iron carboboride $Fe_3(B, C)$. Simultaneously, it is also possible to form boride phases alloyed with carbon, such as Fe(B, C) and $Fe_2(C, B)$ [21–23]. Steel alloyed with carboforming element boron may contain carboboride $Me_{23}(C, B)_6$ [20]. It is suggested that Ni atoms are in the iron-base solid solution and may have I minor effect on the strength properties of the material. When dissolving in ferrite, nickel increases its viscosity.

The solid solution of boron in bcc lattice of iron has a microhardness of 3700 MPa, modified structure α-Fe + Fe_3B has 6300 MPa, eutectic structures of dendrite in commercially pure iron have 6000–16,000 MPa and 40Cr steel 10,000–16,000 MPa. The boride structures in 40Cr steel have the following microhardness: Fe_2B: 16,800 MPa, Fe_2B + FeB: 16,800–18,900 MPa and FeB: 18,900–21,000 MPa [24,25]. Therefore, the high strength properties of the layer surfaced on Hardox 450 steel with wire No.2 may be caused by the formation of eutectic on the basis of iron boride Fe_2B. SEM study of the surfaced layer reveals the formation of lamellar-type eutectic. Its image is presented in Figure 4.

The effect of boron on the properties of iron is similar to that of carbon but is several times stronger. The addition of boron in the quantity of 0.02% (at.) facilitates the refinement of iron grain and gives the possibility to use thermal treatment (quenching) for increasing its properties [22,25]. The results in support of the given thesis were obtained by us when analysing α-phase being formed in eutectic. Figure 5 shows the characteristic image of surfaced layer metal, demonstrating the structure of α-phase interlayer. The lamellar structure is clearly defined. The transverse size of plates varies between 30 and 70 nm. A dislocation substructure of

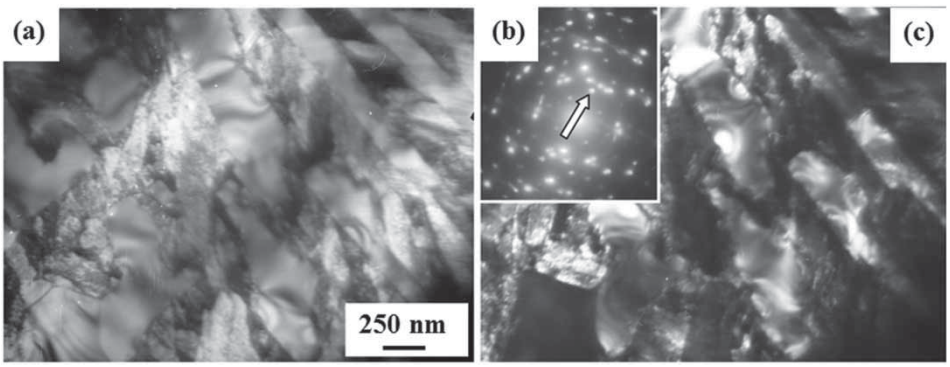

Figure 4. Electron microscope image of structure of the layer surfaced with wire No.2 on Hardox 450 steel ; (a) light field, (b) dark field obtained in closely located reflections [002] Fe_2B and [110]α-Fe and (c) micro-electron diffraction pattern, arrows designate the reflections in which dark field was obtained.

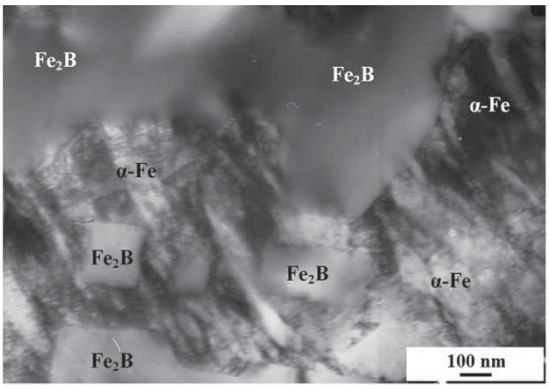

Figure 5. Electron microscope image of structure of the layer surfaced with wire No.2 on Hardox 450 steel.

net-like type is observed in the volume of plates. Judging from the size of dislocation of net cells, the dislocation scalar density amounts to 10^{11} cm^{-2}. The high dislocation density and lamellar morphology of interlayer structure are indicative of the shear mechanism of α-phase formations with the production of ultrafine martensite structure. Note for comparison that the average transverse sizes of plates of packet martensite vary within 150–200 nm in quenched steel, the transverse ones of lamellar martensite crystals reach units of micrometers [19,26].

Carbides and carboborides were not found in the research into the eutectic structure of the surfaced layer; it may be caused by high speeds of material cooling. The presence of hardening martensite with extreme high density of dislocations indicates a high cooling rate of the material. The following tempering of this structure can cause the additional precipitation of caboboride phases.

The less strong structure of the surfaced layer is formed on Hardox 450 steel by applying surfacing wire No.3 (Figure 3, curve 2) and No.1 (Figure 3, curve 3). Hardness of surfaced layer exceeds ≈ 1.7 fold that of the base metal (Hardox 450 steel) and the thickness of surfaced is layer up to 8.0 mm.

When analysing the data presented in Table 2, it may be supposed that the high strength properties of surfaced layer are caused by the strengthening of the material with niobium carbides. System NbC is characterised by the availability of Nb-based solid solution, two stable intermediate phases Nb_2C and NbC, and meta-stable phase Nb_3C_2 [20]. Carbide NbC melts congruently with 46.2 at.-% C content and temperature of 3608 ± 50°C. The wide range of NbC homogeneity is narrowed at temperature decrease and is in the concentration interval of 37–49 at.-% C at temperatures < 3000°C, 41–47 at.-% C at temperatures 1600–2500°C [20]. Carbide NbC has a cubic structure of NaCl type (Pirson symbol cF8, space group Fm3m). With carbon content increase, the parameter of carbide lattice varies within 0.44317–0.44690 nm. Vanadium, being a strong carboforming element, produces a vanadium carbide with carbon of steel in the process of tempering. In addition, the steel alloying with vanadium assists in obtaining the fine-grained structure, the reduction in the tendency to overheating, the softening in tempering and the increase in wear resistance. In our research, the carbides were not found, and it may be caused by the high speed of cooling of surfacing metal in the formation of the surfaced layer.

Carbide Nb_2C is formed as a result of recrystallisation of NbC–Nb_2C at 2500°C. According to most researchers, carbide Nb_2C is formed by the peritectic reaction $Fe + NbC \leftrightarrow Nb_2C$ with content of 34.5 at.-% C and at temperature of 3035 ± 20°C. The Nb_2C homogeneity region at temperature 2000°C is 30.7–32.4 at.-% C. The compound Nb_2C exists in three modifications: α, β and γ. α-Nb_2C has an ordered rhombic structure and it is stable at temperature up to 1200°C, β-Nb_2C – ordered hexagonal structure and exists in the temperature interval 1200–2500°C and γ-Nb_2C – disordered hexagonal structure and it exists at temperatures above 2500°C. The parameters of β-Nb_2C are as follows: $a = 0.3120$–0.3128 nm, $c = 0.4957$–0.4974 nm and $a = 0.3117$–0.3127 nm, $c = 0.4956$–0.4974 nm at 2000°C. Niobium carbide belongs to the hardest hard carbide – 17.3–24.0 GPa [27–29].

The studies of the layer surfaced with wire No.1 and No.2 showed that its high strength properties were caused by the formation of quenched structure (martensite) and precipitation of the second phase particles as well. The characteristic feature of the quenched structure is a coarsening (in comparison with the structure of the layer surfaced with wire No.2) martensite structure, the transverse size of which varies within 100–200 nm (Figure 6).

Indexing of micro-electron diffraction patterns obtained from martensite structure enabled to reveal the presence of retained austenite (γ-phase, solid solution on the basis of face-centred crystal lattice of iron) (Figure 6(b), the reflections of retained austenite are designated by the arrows). The retained austenite in the form of extended interlayers locates along the boundaries of martensite crystals.

The main ordered phase of the layer surfaced with wire No.1 is niobium carbide particles. The size of inclusions varies within 0.2–1.5 µm. The shape of niobium carbide particles is very diverse and it is determined by the place of particle location. In the volume of grains, the niobium carbide particles have, largely, faceted shape (Figure 7(a)); along the boundaries the particles form the extended interlayers (Figure 7(b)); in the grain boundary junctions, they are shaped into triple extended node (Figure 8). In some cases, the reflections belonging to carbides of chromium and tungsten are revealed in micro-electron diffraction patterns.

The layer formed with surfacing wire No.3 contains carbides of complex composition $M_{23}C_6$ as a

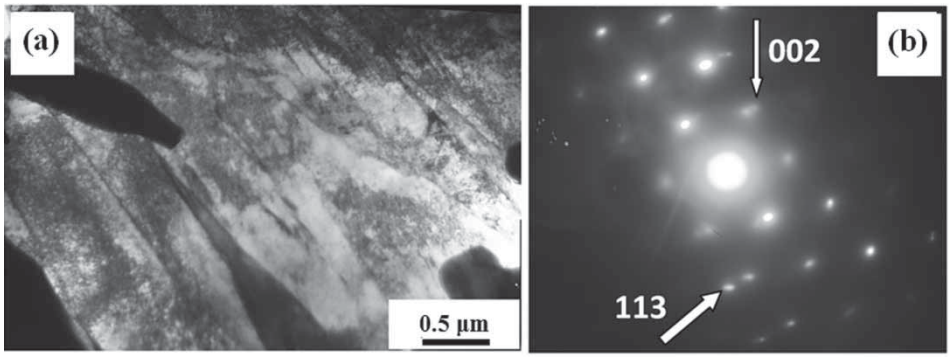

Figure 6. Electron microscope image of α-phase structure of surfacing applied with wire No.3 on Hardox 450 steel. Micrograph shows the γ-phase reflections.

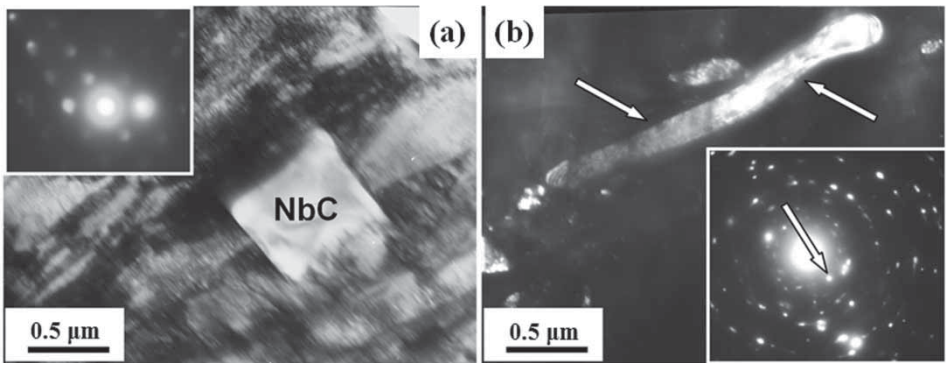

Figure 7. Electron microscope image of surfacing structure applied with wire No.1 on Hardox 450 steel; (a) light field and (b) dark field obtained in reflection [002] NbC (it is designated by the arrow in micro-electron diffraction pattern). In (b) niobium carbide is designated by arrows.

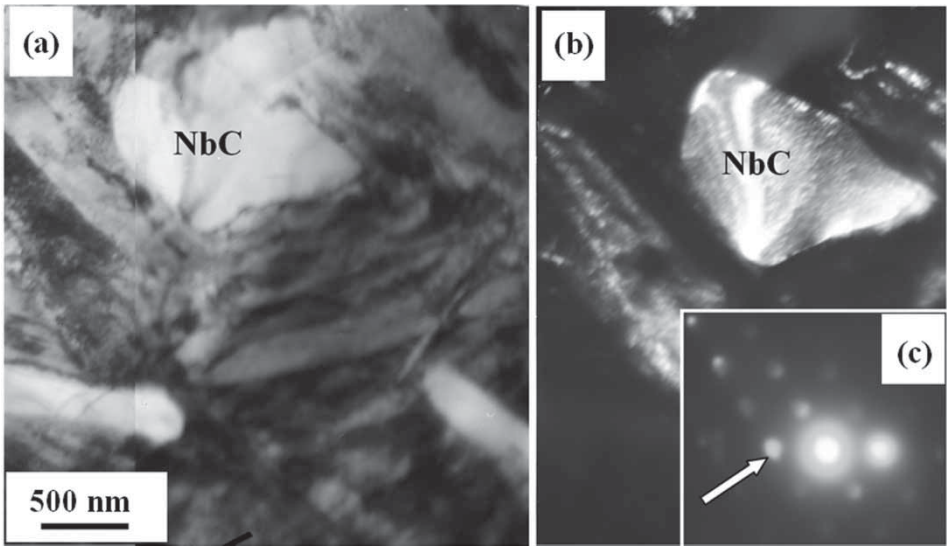

Figure 8. Electron microscope image of surfacing structure applied with wire No.1 on Hardox 450 steel; (a) light field; (b) dark field obtained in closely located reflections [002] NbC+[110]α-Fe (the reflections are designated with arrow in (c)) and (c) micro-electron diffraction pattern, the arrow designates the reflections in which dark field was obtained.

strengthening phase along with niobium carbide NbC. Following the results presented in Table 2, one might expect that carbide under discussion is formed by atoms of chromium, iron and tungsten and it has a composition $(Cr, Fe, W)_{23}C_6$.

Conclusion

(i) The investigation of phase constitution, defect substructure and mechanical properties of the surface layer of Hardox 450 steel surfaced with surfacing

wire No.1, No.2 and No.3 in a single pass is performed.

(ii) It is shown that the highest hardness is the one surfaced with wire No.2. Its strengthened layer thickness is not less than 7.5 mm and its microhardness varies between 10.5 and 12.5 GPa. It is found that the increased mechanical properties of the surfaced layer are connected to the formation of multi-phase submicro and nanoscale structures.

(iii) The strengthening is caused by the quenching-induced formation of ultra-fine martensite and the presence of the inclusions mainly of iron boride Fe_2B of submicron size and the formation of the eutectic of the lamellar structure.

Disclosure statement

No potential conflict of interest was reported by the authors.

Funding

Financial support of the research was provided in part under grant of Russian Science Foundation [project No. 15-19-00065].

ORCID

Sergey Konovalov http://orcid.org/0000-0003-4809-8660

References

[1] Atamert S. Stability, wear resistance, and microstructure of iron, cobalt and nickel-based hardfacing alloys [Ph.D thesis]. Cambridge: University of Cambridge; 1989.

[2] Arulmani R, Sunil P. Surfacing applications – a review. National Workshop on Welding Technology, SLIET, Longowal; April 2003; 233–238.

[3] Kirchgaßner M, Badisch E, Franek F. Behaviour of iron-based hardfacing alloys under abrasion and impact. Wear. 2008;265(5–6):772–779.

[4] Budinski KG. Surface engineering for wear resistance. Upper Saddle River (NJ): Prentice Hall; 1988.

[5] Mendez PF, Barnes N, Bell K, et al. Welding processes for wear resistant overlays. J Manuf Process. 2014;16(1):4–25.

[6] Zahiri R, Sundaramoorthy R, Lysz P, et al. Hardfacing using ferro-alloy powder mixtures by submerged arc welding. Surf Coat Technol. 2014;260:220–229.

[7] Budinski KG. Hardfacing: an overview of the processes. Weld Design Fabr. 1986;51–57.

[8] Wu W, Hwu LY, Lin DY, et al. The relationship between alloying elements and retained austenite in martensitic stainless steel welds. Scr Mater. 2000;42(11): 1071–1076.

[9] Antony KC, Glenny J, Northwood JE. Hard facing, welding, brazing and soldering. 9th ed. Vol. 6, 'Metals Hand book', 1983, American Society for Metals.

[10] Yılmaz O, Özenba M, Buytoz S. Microstructural characteristics of gas tungsten arc synthesised Fe-Cr-Si-C coating. Mater Sci Technol. 2002;18(10):1209–1216.

[11] Komvopoulos K, Nagarathnam K. Processing and characterization of laser-cladded coating materials. J Eng Mater Technol. 1990;112(2):131–143.

[12] Agarwal A, Dahotre NB. Comparative wear in titanium diboride coatings on steel using high energy density processes. Wear. 2000;240(1–2):144–151.

[13] Teker T, Karataş S, Osman Yilmaz S. Microstructure and wear properties of AISI 1020 steel surface modified by HARDOX 450 and FeB powder mixture. Prot Metals Phys Chem Surf. 2014;50(1):94–103.

[14] Kapralov EV, Raykov SV, Budovskikh EA, et al. Structural-phase states and properties of coatings welded onto steel surfaces using powder. Bull Russ Acad Sci Phys. 2014;78(10):1015–1021.

[15] Raikov SV, Kapralov EV, Ivanov YF, et al. Structure gradient in wear-resistant coatings on steel. Steel Transl. 2015;45(2):120–124.

[16] Raykov SV, Kapralov EV, Vashchuk ES, et al. Structure of the surface layer of a wear-resistant coating after treatment with a high-intensity electron beam. J Surf Invest X-Ray Synchrotron Neutron Technol. 2015;9(5):934–938.

[17] Popova N, Nikonenko E, Ivanov Y, et al. Structure and properties of wear-resistant weld deposit formed on martensitic steel using the electric-arc method. Adv Mater Res. 2014;1013:194–199.

[18] Kapralov EV, Raikov SV, Vaschuk ES, et al. Structural-phase states and wear resistance of surface formed on steel by surfacing. AIP Conf Proc. 2014;1623:233–236.

[19] Kurduymov VG, Utevskii LM, Entin RI. Transformation in iron and steel. Moscow: Nauka; 1977.

[20] Bannykh OA, Budberg PB, Alisova SP. State diagrams of binary and multi-component systems on base of iron. Moscow: Metallurgiya; 1986.

[21] Spiridonova IM, Sukhovaya EV, Balakin VP. Structure and peculiarities of Fe(B,C) crystals. Metallurgia. 1996;35(2):65–68.

[22] Sukhovaya EV. Regularities of structure and properties of iron boride base solid solutions. Vestnik Dnepropetrovsk Univ. 2008;16(15):106–110.

[23] Spiridonova IM, Sukhovaya EV, Sergeev G. Phase transformations in high boride iron alloys alloyed with carbon. Teoria praktica metallurgii. Special Issue. Eutectica VII. 2006;53–54(4–5):57–59.

[24] Biryukov V. Modification of surface with the help of laser radiation. Fotonika. 2010;3:18–21.

[25] Lakhtin YM, Kogam YD, Buryukin AV. Surface saturation of steel with boron by application of laser radiation. Metall Heat Treat Metals. 1985;11:9–11.

[26] Ivanov YF, Kornet EV, Kozov EV, et al. Quenched structural steel: structure and mechanisms of hardening. Novokuznetsk: SibSIU; 2010.

[27] Hasui A, Morigakio O. Surfacing and spraying. Moscow: Mashinostroenie; 1985.

[28] Goldstein MI, Farber VM. Dispersion hardening of steel. Moscow: Metallurgia; 1979.

[29] Samsonov GV, Umanski YaS. Solid compounds of high-melting metals. Moscow: Metallurgizdat; 1957.